The interaction of planets with a disc with MHD turbulence IV: Migration rates of embedded protoplanets

Richard P. Nelson & John C.B. Papaloizou
Astronomy Unit, Queen Mary, University of London, Mile End Rd, London E1 4NS

Received/Accepted

ABSTRACT

We present the results of global cylindrical disc simulations and local shearing box simulations of protoplanets interacting with a disc undergoing MHD turbulence. The specific emphasis of this paper is to examine and quantify the magnitude of the torque exerted by the disc on the embedded protoplanets as a function of the protoplanet mass, and thus to make a first study of the induced orbital migration of protoplanets resulting from their interaction with magnetic, turbulent discs. This issue is of crucial importance in understanding the formation of gas giant planets through the so–called core instability model, and the subsequent orbital evolution post formation prior to the dispersal of the protostellar disc. Current estimates of the migration time of protoplanetary cores in the 3 – 30 Earth mass range in standard disc models are $\tau_{mig} \simeq 10^4$ – 10^5 yr, which is much shorter than the estimated gas accretion time scale of Jupiter type planets.

The global simulations were carried out for a disc with aspect ratio $H/R = 0.07$ and protoplanet masses of $M_p = 3, 10$, 30 Earth masses, and 3 Jupiter masses. The local shearing box simulations were carried out for values of the dimensionless parameter $(M_p/M_*)/(H/R)^3 = 0.1, 0.3, 1.0$, and 2.0, with M_* being the central mass. These allow both embedded and gap forming protoplanets for which the disc response is non linear to be investigated.

In all cases the instantaneous net torque experienced by a protoplanet showed strong fluctuations on an orbital time scale, and in the low mass embedded cases oscillated between negative and positive values. Consequently, in contrast to the laminar disc type I migration scenario, orbital migration would occur as a random walk. Running time averages for embedded protoplanets over typical run times of 20 – 25 orbital periods, indicated that the averaged torques from the inner and outer disc took on values characteristic of type I migration. However, large fluctuations occurring on longer than orbital time scales remained, preventing convergence of the average torque to well defined values or even to a well defined sign for these lower mass cases.

Fluctuations became relatively smaller for larger masses indicating better convergence properties, to the extent that in the $30M_\oplus$ simulation consistently inward, albeit noisy, migration was indicated.

Both the global and local simulations showed this trend with increasing protoplanet mass which is due to its perturbation on the disc increasing to become comparable to and then dominate the turbulence in its neighbourhood. This then becomes unable to produce very large long term fluctuations in the torques acting on the protoplanet. Eventually gap formation occurs and there is a transition to the usual type II migration at a rate determined by the angular momentum transport in the distant parts of the disc.

The existence of significant fluctuations occurring in the turbulent discs on long time scales is an important unexplored issue for the lower mass embedded protoplanets, that are unable to modify the turbulence in their neighbourhood, and which have been studied here. If significant fluctuations occur on the longest disc evolutionary time scales, convergence of torque running averages for practical purposes will not occur and the migration behaviour of low mass protoplanets considered as an ensemble would be very different from predictions of type I migration theory for laminar discs. The fact that noise levels were relatively smaller in the local simulations may indicate the presence of long term global fluctuations, but the issue remains an important one for future investigation.

Key words: accretion, accretion disks — MHD, instabilities, turbulence – planetary systems: formation, protoplanetary discs

1 INTRODUCTION

The ongoing discovery of extrasolar giant planets has stimulated renewed interest in the theory of planet formation (e.g. Mayor & Queloz 1995; Marcy, Cochran, & Mayor 1999; Vogt et al. 2002; Santos et al. 2003). In the most commonly accepted theory of how planets form, the so–called core instability model, gas giant planets form through the build–up of a rocky and icy core of ~ 15 Earth masses, which then undergoes gas accretion resulting in a gas–giant planet (e.g. Bodenheimer & Pollack 1986; Pollack et al. 1996). An alternative model involves the formation of giant planets through the gravitational fragmentation of the protostellar disc during the earlier phases of its evolution (Boss 2001). In either case disc–planet interaction will play an important role in the subsequent evolution.

The gravitational interaction between protostellar discs and embedded protoplanets has been the subject of a large number of studies over the last couple of decades. In the standard picture, a protoplanet exerts torques on a protostellar disc through the excitation of spiral density waves at Lindblad resonances, and possibly through interaction at corotation resonance (e.g. Goldreich & Tremaine 1979; Lin & Papaloizou 1979; Papaloizou & Lin 1984; Ward 1986, 1997; Tanaka, Tacheuchi & Ward 2002). The spiral waves carry with them an associated angular momentum flux. This angular momentum is deposited in the disc material where the waves are damped, leading to an exchange of angular momentum between protoplanet and disc. The disc that lies exterior to the protoplanet orbit exerts a negative torque on the planet, and the interior disc exerts a positive torque. For most disc models the negative torque dominates and the protoplanet migrates inwards. For protoplanets of ~ 15 Earth masses, the migration time is estimated to be between 10^4 and 10^5 yr (Tanaka, Tacheuchi, & Ward 2002), which is very much shorter than the estimated gas accretion phase of giant planet formation $\simeq 7$ Myr (Pollack et al. 1996). Taken at face value, this presents a serious problem for the core–instability model of gas giant planet formation. We note, however, this analysis pertains only to smooth, laminar disc models.

For protoplanets in the Jovian mass range, the interaction is non linear and gap formation occurs (Papaloizou & Lin 1984; Bryden et al. 1999; Kley 1999). In this case the orbital migration of the planet becomes locked to the viscous evolution of the disc, and migration is expected to occur on a time scale of 10^5 yr (Lin & Papaloizou 1986; Nelson et al. 2000; D'Angelo, Kley & Henning 2002).

Until quite recently most models of viscous accretion discs used the Shakura & Sunyaev (1973) α model for the anomalous disc viscosity. This assumes that the viscous stress is proportional to the thermal pressure in the disc, without specifying the origin of the viscous stress (but assumed to arise from some form of turbulence). Work by Balbus & Hawley (1991) indicated that significant angular momentum transport in weakly magnetised discs could arise from the magnetorotational instability (MRI – or the Balbus–Hawley instability). Subsequent non linear numerical simulations performed using a local shearing box formalism (e.g. Hawley & Balbus 1991; Hawley, Gammie, & Balbus 1996; Brandenburg et al. 1996) confirmed this and showed that the saturated non linear outcome of the MRI is MHD turbulence with an associated viscous stress parameter α of between $\sim 5 \times 10^{-3}$ and ~ 0.1, depending on the initial magnetic field configuration. More recent global simulations of MHD turbulent discs [e.g. Armitage 1998; Hawley 2000; Hawley 2001; Steinacker & Papaloizou 2002; Papaloizou & Nelson 2003] confirm the picture provided by the local shearing box simulations.

This is the fourth in a series of papers that examine the interaction between disc models undergoing MHD turbulence with zero net flux magnetic fields and embedded protoplanets. In Papaloizou & Nelson (2003 – hereafter paper I) we examined and characterised the turbulence obtained in a variety of MHD disc models. In Nelson & Papaloizou (2003 – hereafter paper II) we examined the interaction between a global cylindrical disc model and a massive (5 Jupiter mass) protoplanet. A similar study was undertaken by Winters, Balbus, & Hawley (2003b). In a companion paper to this one (Papaloizou, Nelson, & Snellgrove 2003 – hereafter paper III) we presented the results of global cylindrical disc simulations and local shearing box simulations of turbulent discs interacting with protoplanets of different mass. The main focus of paper III was to characterise the changes in flow morphology and disc structure as a function of planet mass, and to examine the transition from linear to non linear interaction leading to gap formation. In this paper we continue to examine these simulations, but now focus on the gravitational torques exerted on the protoplanet by the disc and the associated migration rate of the protoplanet. The migration of low mass planets in *strongly* magnetised, non–turbulent discs has recently been considered by Terquem (2003), who found that migration could be significantly modified and even reversed under favourable conditions. In this paper we consider the migration of planets in *weakly* magnetised, turbulent disc models only.

We find that in all simulations performed, the torque experienced by the protoplanet is a highly variable quantity on account of the protoplanet interacting with the turbulent density wakes that shear past it. For low mass protoplanets, the torque is dominated by these fluctuations, such that the usual distinction between inner (positive) and outer (negative) disc torques is blurred. The net torque experienced by embedded protoplanets oscillates between negative and positive values, such that the protoplanet migration is likely to occur as a random walk. This is in contrast to the monotonic inward drift normally associated with type I migration. A running time average of the torques fails to converge for the embedded protoplanet runs, at least for the run times that are currently feasible, so that definitive statements about the direction and rate of migration of low mass planets in turbulent discs cannot yet be made.

In a manner that is consistent with the results of paper III, we find that the results show a definite trend as a function of planet mass. For very low mass planets the turbulent density wakes are of much higher amplitude than the spiral wakes generated by the planet. This is reflected in the torque experience by the planet, for which the turbulent fluctuations are very much larger than the running mean torque. As the planet mass increases, the spiral wakes generated by the planet become apparent in the flow. This is accompanied by the torques displaying the expected separation between inner and outer disc torques, and the fluctuations becoming smaller relative to the running mean torque. This trend

with increasing mass continues until gap formation occurs. At this point we find a weakening of the torques exerted by the disc on the protoplanet due to the evacuation of gap material. There is then a transition to type II migration and, as exemplified by the simulation of a 5 Jupiter mass protoplanet interacting with a turbulent disc presented in paper II, inward migration at a rate determined by the angular momentum transport in the distant parts of the disc unaffected by the protoplanet.

The plan of the paper is as follows. In section 2 we described our initial model set up and numerical procedure. In section 3 we present the results of the simulations. Finally in section 4 we discuss our results.

2 INITIAL MODEL SETUP

The initial set up and boundary conditions used in the models presented in this paper are described in detail in paper III, and we do not repeat that discussion here. However, we present some details of the runs in tables 1 and 2 for convenience. Table 1 contains details of the global runs, and table 2 contains details of the local shearing box runs.

2.1 Global Runs

The initial conditions for the global runs consisted of a turbulent accretion disc model with $H/r = 0.07$, H being the putative disc semi thickness, and a volume averaged characteristic Shakura–Sunyaev α value of $\alpha \simeq 7 \times 10^{-3}$, as described in paper III. At time $t = 0$ the protoplanet was inserted into the disc and subsequently held fixed at location $(r_p, \phi_p) = (3, \pi)$ in cylindrical coordinates (r, ϕ) centred on the central mass M_*. The gravitational potential of the protoplanet was softened using a softening parameter $b = 0.3H_p$, where H_p is the disc scale height at the planet location. The simulation was performed in a rotating reference frame whose angular velocity equalled the Keplerian angular velocity of the protoplanet. The torque on the planet as a function of time was calculated in the manner described in section 2.4. The unit of time used when discussing the global runs is the orbital period of the protoplanet $P_p = 2\pi/\Omega_p$.

2.2 Shearing Box Runs

The morphology of the shearing box runs has already been described in detail in paper III. These were generated from a simulation Ba0 described there which had fully developed turbulence, but no protoplanet, that had been run for 354 time units. The time unit was taken to be the inverse angular velocity ,Ω_p, at the centre of the box located a putative distance R from the central object. Simulations Ba1–Ba4 were then carried out after inserting protoplanets with a range of values for $GM_p/(H^3\Omega_p^2) = M_pR^3/(M_*H^3)$, with M_p being the protoplanet mass. These and other relevant parameters are given in table 2. As for the global simulations, the protoplanet potential was softened, by use of a softening parameter $b = 0.3H$. For additional details see paper III. The results of these simulations are presented in section 3.6.

2.3 Numerical procedure

The numerical scheme that we employ is based on a spatially second–order accurate method that computes the advection using the monotonic transport algorithm (Van Leer 1977). The MHD section of the code uses the method of characteristics constrained transport (MOCCT) as outlined in Hawley & Stone (1995) and implemented in the ZEUS code. The code has been developed from a version of NIRVANA originally written by U. Ziegler (Ziegler & Rudiger 2000).

2.4 Torque Calculation

The torque experienced by the protoplanet in the global disc runs was calculated by summing the gravitational force due to the mass in each grid cell in the active domain of the disc model. Those cells that lay within the boundary layers located near the radial boundaries of the computational domain (described in paper III) did not contribute to the gravitational force. The gravitational force due to the protoplanet acting on the disc was softened using $b = 0.3H_p$ where H_p is the putative scale height at the position of the protoplanet. An identical softening was used when calculating the force of the disc on the protoplanet. Material that lay inside the Hill sphere of the protoplanet given by $R_H = r_p(M_p/3M_*)^{1/3}$ was excluded from the torque calculation. The acceleration experienced by the protoplanet can be written as

$$\mathbf{f} = \sum_{i=1}^{N_{cells}} -\frac{G\, m_i\, (\mathbf{r}_p - \mathbf{r}_i)}{(r_p^2 + r_i^2 - 2r_p r_i \cos(\phi_p - \phi_i) + b^2)^{3/2}}$$

where the sum is over all possible values of the subscript i which is used to label quantities evaluated at the centre of a specific grid cell, thus ensuring that the whole of the computational domain is covered. The mass in each grid cell $m_i = \rho_i \Delta r\, r_i\, \Delta\phi\, \Delta z$, where Δr, $\Delta\phi$, and Δz are the grid spacings in the radial, azimuthal, and vertical directions respectively. The resulting torque per unit mass is then $\mathbf{T} = \mathbf{r}_p \times \mathbf{f}$. This quantity was calculated and stored every 10 time steps.

A similar procedure was used to calculate the force acting on the planet in the shearing box simulations.

3 NUMERICAL RESULTS

Before discussing the results of the global turbulent disc simulations, we present the results of some simulations designed to calibrate the code. In particular, we will examine the role that gravitational softening of the protoplanet gravitational potential has on the migration time in laminar disc simulations.

3.1 Type I migration in laminar discs

The migration time of a non gap forming protoplanet embedded in a three dimensional disc has been calculated using a linear analysis by Tanaka, Takeuchi, & Ward (2002). They derive the following expression for the migration time of a protoplanet embedded in a locally isothermal disc with a power law surface density profile:

Model	ϕ domain	H/r	M_p/M_*	$(M_pR^3/(M_*H^3)$	n_r	n_ϕ	n_z
G1	2π	0.07	1×10^{-5}	0.03	450	1092	40
G2	2π	0.07	3×10^{-5}	0.09	450	1092	40
G3	2π	0.07	1×10^{-4}	0.30	450	1092	40
G4	2π	0.07	3×10^{-3}	8.75	450	1092	40
G5	$\pi/2$	0.07	3×10^{-3}	8.75	450	276	40

Table 1. Parameters of the global simulations: The first column gives the simulation label, the second gives the extent of the azimuthal domain, the third gives the H/r value of the disc, and the fourth gives the protoplanet-star mas ratio. The fifth gives the ratio of M_p/M_* to $(H/r)^3$. The sixth, seventh, and eighth columns describe the number of grid cells used in each coordinate direction.

Model	z domain	x domain	y domain	t_1	t_2	$(M_pR^3/(M_*H^3)$	n_z	n_x	n_y
Ba1	$(-H/2, H/2)$	$(-4H, 4H)$	$(-2\pi H, 2\pi H)$	354	621	0.1	35	261	200
Ba2	$(-H/2, H/2)$	$(-4H, 4H)$	$(-2\pi H, 2\pi H)$	354	644	0.3	35	261	200
Ba3	$(-H/2, H/2)$	$(-4H, 4H)$	$(-2\pi H, 2\pi H)$	354	619	1.0	35	261	200
Ba4	$(-H/2, H/2)$	$(-4H, 4H)$	$(-2\pi H, 2\pi H)$	354	650	2.0	35	261	200

Table 2. Parameters of the shearing box simulations: The first column gives the simulation label, the second, third and fourth give the extent of the coordinate domains considered. The x, y, and z domains refer to the Cartesian domains labeled as radial, azimuthal and vertical respectively. The fifth and sixth column give the start and end times if the simulation measured in dimensionless units described in section 2.2. These were all started by inserting the protoplanet into the turbulent model generated from the simulation Ba0 described in paper III at time indicated. The seventh column gives the value of $(GM_p/(\Omega_p^2H^3) = (M_pR^3/(M_*H^3)$. The eighth, ninth and tenth columns give the number of computational grid points in the x, y, and z coordinates respectively. These numbers include any ghost zones used to handle boundary conditions.

$$\tau_{mig} = (2.7 + 1.1\gamma)^{-1} \frac{M_*}{M_p} \frac{M_*}{\Sigma_p r_p^2} \left(\frac{c}{r_p \Omega_p} \right)^2 \Omega_p^{-1} \qquad (1)$$

Here Σ_p is the surface density at the position of the protoplanet, Ω_p is the Keplerian angular velocity of the protoplanet, c is the sound speed in the disc at the protoplanet position, and $-\gamma$ is the power law index for the radial surface density distribution. These authors comment that in general this expression gives a migration time that is a factor of between $2-3$ times slower than similar expressions derived for flat, two–dimensional discs (e.g. Ward 1997). The finite disc thickness thus acts to soften the disc–planet gravitational interaction.

The global turbulent disc simulations presented here use cylindrical disc models in which the vertical component of gravity is neglected, and thus the full three dimensional structure of the disc is not modeled. In the limit of a laminar disc, the cylindrical disc can be viewed as a series of two dimensional discs stacked on top of one another, providing the protoplanet gravitational potential is also cylindrical (i.e. no vertical component). Given that gravitational softening of the protoplanet potential is employed, we are interested in (*i*) How large a gravitational softening is required in a two dimensional disc simulation to obtain agreement with equation 1; (*ii*) What is the deviation from equation 1 obtained for differing softening parameters. In order to address these points a number of two dimensional simulations using laminar, viscous α–discs have been performed with varying physical and softening parameters.

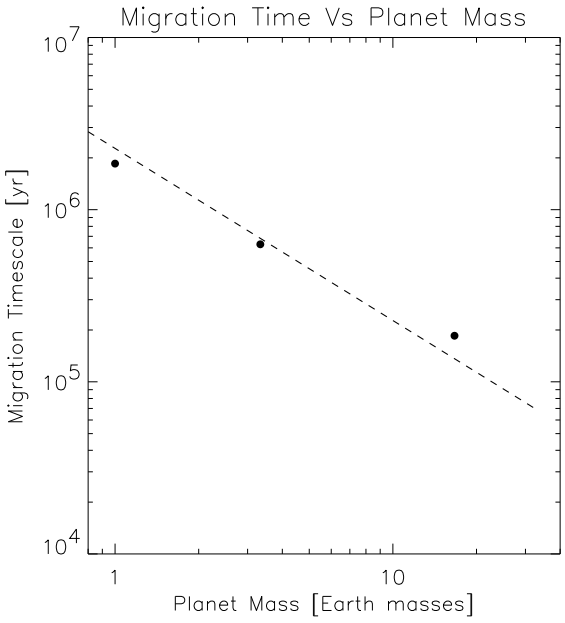

Figure 1. This figure shows the migration time for protoplanets of different mass using a gravitational softening parameter $b = 0.7H_p$. The dots show the results of the simulations, and the dashed line shows the migration time computed from equation 1.

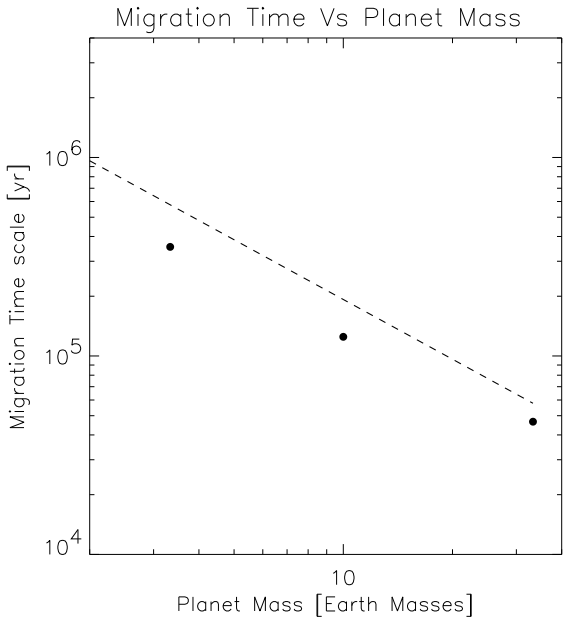

Figure 2. This figure shows the migration time for protoplanets of different mass using a gravitational softening parameter $b = 0.3H_p$. The dots show the results of the simulations, and the dashed line shows the migration time computed from equation 1.

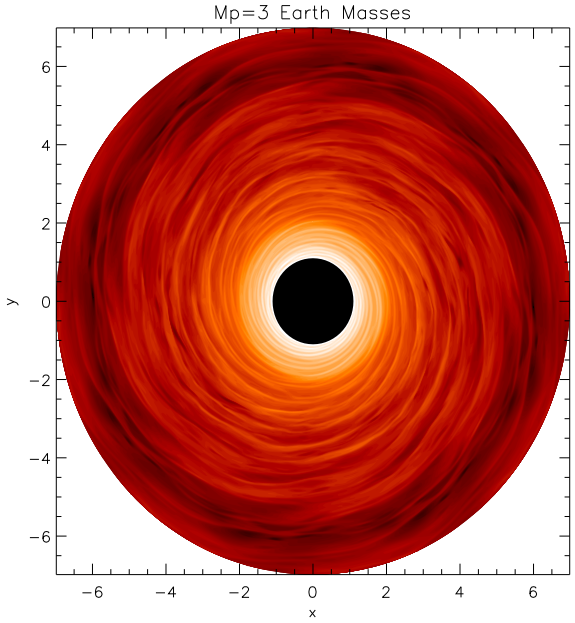

Figure 3. This figure shows midplane density contours for the run G1. Note that the presence of the protoplanet is undetectable due to the higher amplitude perturbations generated by the turbulence. The protoplanet is located at (x_p,y_p)= (-3,0).

Figure 1 shows the migration time for a series of models in which protoplanets of differing masses were placed in a protostellar disc model and the torque of the disc acting on the protoplanet was calculated. These torques were then used to calculate a migration time using the expression

$$\tau_{mig} = \frac{r_p}{\dot{r}_p} = \frac{1}{2}\frac{j_p}{T_p} \qquad (2)$$

where j_p is the specific angular momentum of the protoplanet and T_p is the torque per unit mass due to the disc. The disc model used for the particular set of simulations presented in figure 1 was such that the disc surface density $\Sigma(r) = \Sigma_0 r^{-1/2}$, $H/r = 0.05$, and the dimensionless viscosity coefficient $\alpha = 4 \times 10^{-3}$. In code units the inner boundary was located at $R_{in} = 1$, the outer boundary at $R_{out} = 8$, and the protoplanet was located at $r_p = 3$. If we use the convention that r_p is equivalent to 5.2 AU, and the central stellar mass is a solar mass, then the disc mass was normalised so that it contained the equivalent of 7.5 Jupiter masses between 1.56 and 20.8 AU. This disc model is equivalent to that described in Bate et al. (2003), and figure 1 is directly comparable with their figure 10. The gravitational softening parameter was set to be $b = 0.7H_p$ where H_p is the disc thickness at the position of the protoplanet. We use the convention that 1 Earth mass corresponds to $M_p/M_* = 3 \times 10^{-6}$.

The black dots in figure 1 show the migration time scales obtained in the simulation. The dashed line is obtained from equation 1 assuming an identical disc model. It is clear that a gravitational softening parameter of $b = 0.7H_p$ gives good agreement with the migration time appropriate to a fully three dimensional locally isothermal disc, and that two dimensional simulations can be used to study the migration of low mass protoplanets provided an appropriate gravitational softening parameter is used.

Figure 2 shows the migration time calculated for simulations in which $\Sigma(r) \propto r^{-1}$, $H/r = 0.07$, and the softening parameter was $b = 0.3H_p$. These are the values adopted for the global turbulent disc runs presented in sections 3.2, 3.3, and 3.4, because the potential is better represented close to the planet. The disc model here was normalised so that it contained the equivalent of 0.02 $M_\odot$ between 0 and 40 AU, and $\simeq$ 2.5 Jupiter masses interior to the protoplanet radius r_p. Figure 2 shows that this results in migration times that are a factor of $\simeq 2/3$ shorter than those predicted by Tanaka, Tacheuchi, & Ward (2002) for the smaller masses but are in slightly closer agreement in the higher $\sim 30M_\oplus$ range. These shorter migration times arise because of the smaller softening parameter employed.

3.2 Global Model G1

The global model G1 described in table 1 contained a protoplanet whose mass is equivalent to $\simeq$ 3 Earth masses. Such a protoplanet is expected to provide a small perturbation to the disc. A snapshot of the midplane density is shown in figure 3, and shows that the presence of the protoplanet is indiscernible due to the higher amplitude density fluctuations generated by the turbulence. Figure 4 shows a series of close–up images of the midplane density in the near vicinity of the protoplanet, which again show that the protoplanet cannot be detected. A similar plot for an equivalent laminar disc run is presented in figure 5 for purposes of comparison. It is worth noting that once the density structure shown in figure 5 is established in the laminar disc runs, it remains essentially time independent. The changing density structure observed in figure 4, combined with the larger amplitude of

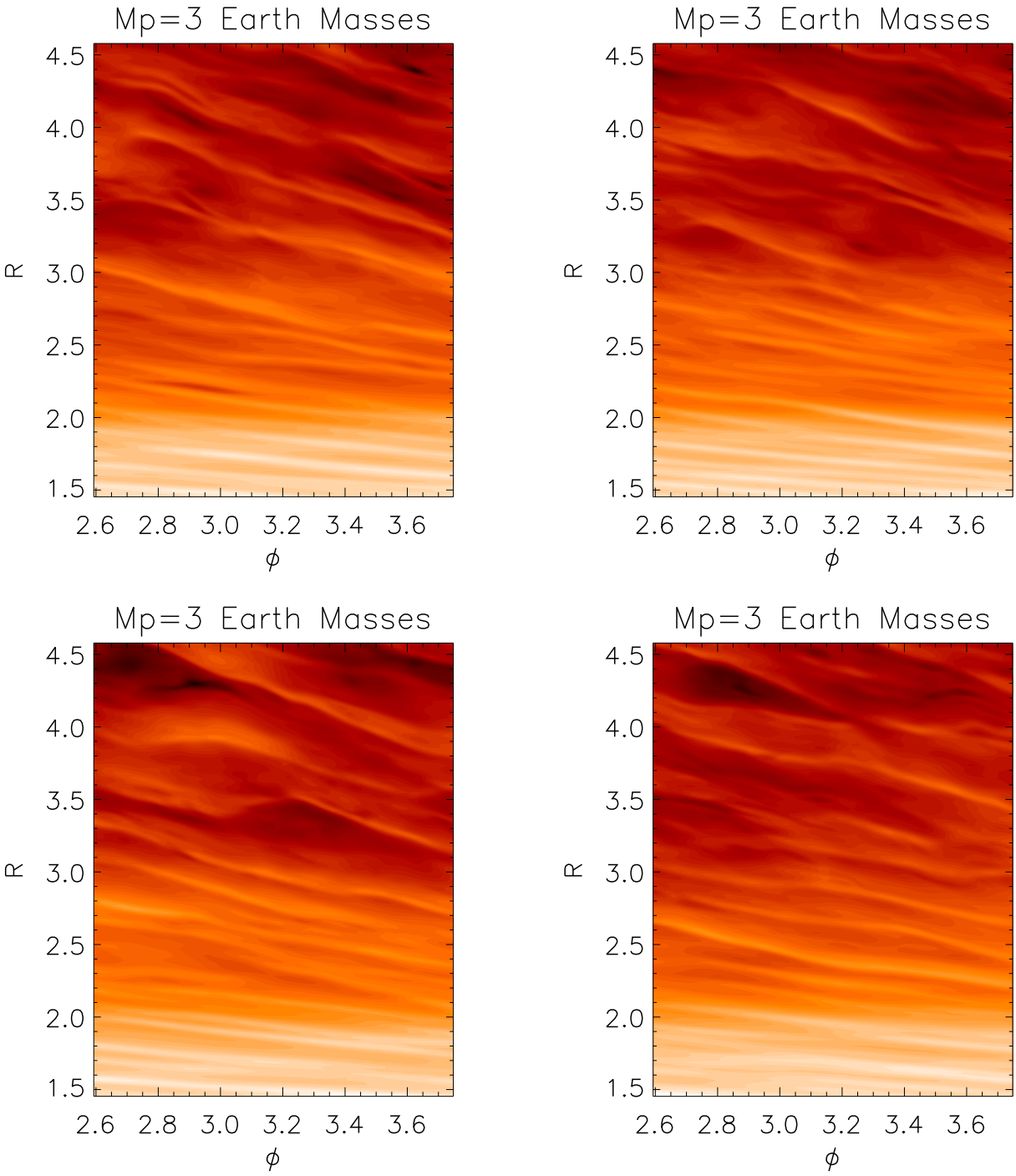

Figure 4. This figure shows midplane density contours for the run G1 in the region close to the protoplanet. The protoplanet is located at $(r_p,\phi_p)= (3,\pi)$. The panels correspond to times 452.4903, 497.7334, 542.9972, and 672.4058, respectively. Note that the presence of the protoplanet is undetectable due to the higher amplitude perturbations generated by the turbulence.

the turbulent wakes when compared with those generated by the protoplanet, suggest that the gravitational interaction between a low mass protoplanet and turbulent disc may differ substantially when compared with a laminar disc.

Figure 6 shows the time evolution of the torque per unit mass exerted on a protoplanet of equivalent parameters to that in run G1 but embedded in a laminar disc. The upper line shows the (positive) torque due to the disc lying interior to the protoplanet orbital radius, the lowest line shows the torque due to the outer disc, and the middle line shows the total (negative) torque. It is clear that a well defined net torque acting on the protoplanet may be defined, along with a corresponding inward migration rate.

Figure 7 shows a similar plot but for the turbulent disc

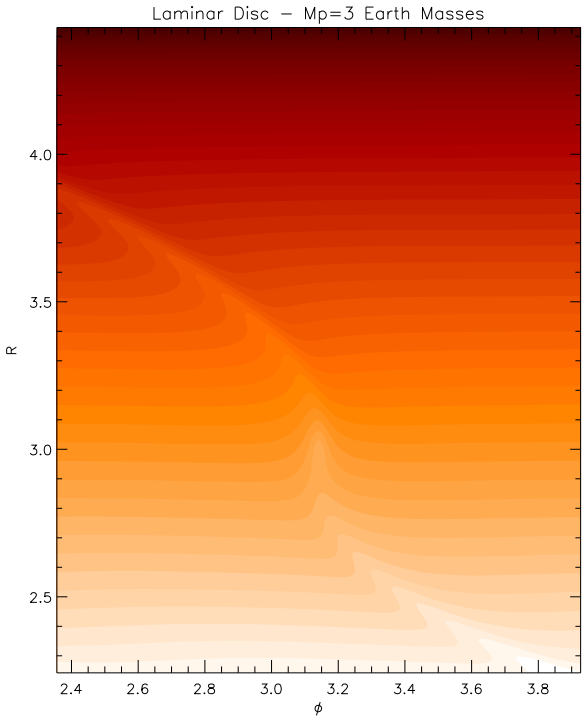

Figure 5. This figure shows midplane density contours for a laminar disc run with planet parameters identical to run G1. The presence of the planet due to the excitation of spiral waves is clearly detectable, in contrast to the picture presented in figure 4.

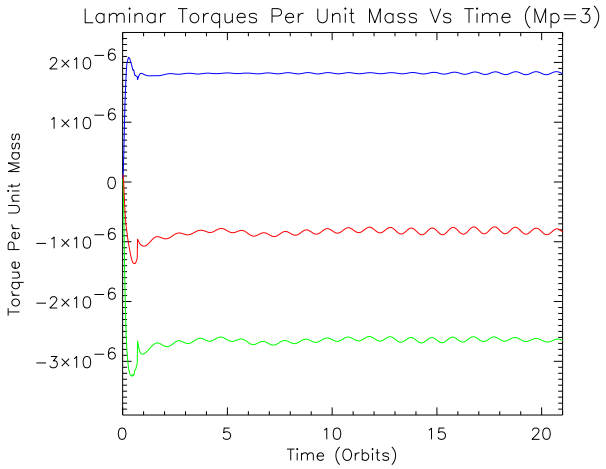

Figure 6. This figure shows the torque per unit mass exerted by the disc on the protoplanet for a laminar disc and planet parameters identical to run G1. The upper line shows the torque due to the inner disc, the lower line shows the torque due to the outer disc, and the middle line shows the total torque. It is clear that a well defined net torque is produced, with an associated migration time scale.

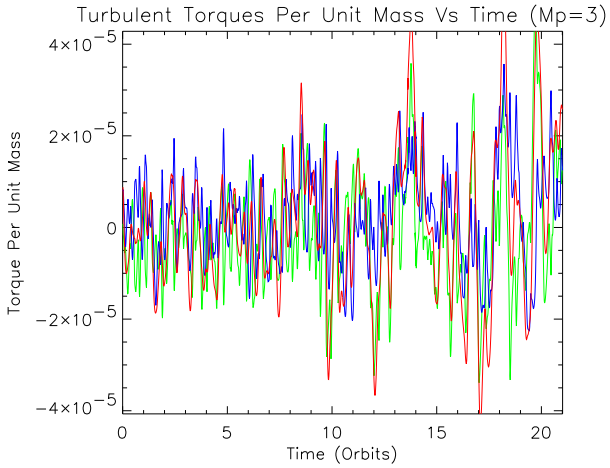

Figure 7. This figure shows the torque per unit mass exerted by the disc on the protoplanet for the run G1. The turbulence in this case generates strong fluctuations in the torque from each side of the disc, such that it becomes difficult to distinguish the torques arising from each side. The total torque fluctuates between positive and negative values such that the associated migration will undergo a 'random walk'.

model G1. It is clear that the forcing experienced by the protoplanet in this case differs dramatically from that obtained in the laminar disc. The torques from the inner and outer disc suffer very large fluctuations as a result of the protoplanet interacting gravitationally with the turbulent wakes apparent in figures 3 and 4 as they shear past the protoplanet, and this causes the net torque experienced by the protoplanet to oscillate between negative and positive values. The orbital migration of the protoplanet is thus likely to occur as a random walk rather than as a monotonic inward drift normally associated with type I migration. In this run, for which the spiral wakes generated by the planet are completely dominated by the turbulent wakes, the usual separation between inner and outer disc torques is barely discernible due to the high amplitude turbulent fluctuations.

The time evolution of the running time average of the torque per unit mass in model G1 is shown in figure 8. The upper line shows the running time average of the torque due to the inner disc, the lowest line shows the time averaged torque due to the outer disc, and the middle line shows the running time average of the total torque. The straight line shows the time average of the total torque per unit mass experienced in an equivalent laminar disc model. The first thing to note from figure 8 is that the running time averaged torque in run G1 does not converge to a well defined value for the time over which the simulation was run (just over 20 planet orbits). Near the beginning of the simulation the time average is close to that obtained from a similar laminar disc run, but as the calculation evolves the running time average changes continuously. By the end of the simulation, the torque experienced by the protoplanet will be positive on average, corresponding to outward migration on a time scale of $\simeq 2.8$ Myr.

If we assume that there exists a well defined long term mean for the torque experienced by the protoplanet, then we can express the torque as the sum of this mean torque and a fluctuating component:

$$T(t) = \overline{T} + T_f(t) \tag{3}$$

where $T(t)$ is the torque experienced at time t, $\overline{T}$ is the mean torque, and $T_f(t)$ is the fluctuating component. The running time average of the torque is given by

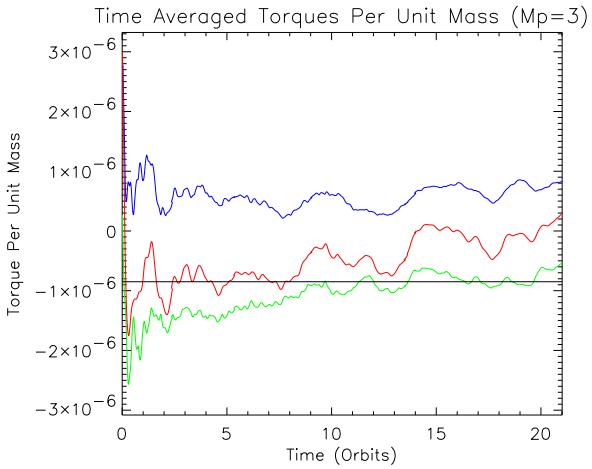

Figure 8. This figure shows the running time average of the torque per unit mass exerted by the disc for run G1. The upper line is the running time average of the torque acting on the planet due to the inner disc. The lower line is that due to the outer disc. The middle (not straight) line is the running time average of the total torque. The straight line is the total torque exerted on the protoplanet in a laminar disc run. We note that the total time averaged torque does not converge to a well defined value.

$$\langle T\rangle_t = \frac{\int_0^t T(t)dt}{\int_0^t dt} \tag{4}$$

then we can write

$$\langle T\rangle_t = \overline{T} + \frac{1}{t}\int_0^t T_f(t)dt. \tag{5}$$

Assuming that the amplitude of the torque fluctuations $T_f(t)$ about the mean $\overline{T}$ follow a Gaussian distribution with standard deviation σ_T and recur on a characteristic timescale t_f, we can estimate from equation 5 that the fluctuations in the running mean satisfy

$$|\langle T_t\rangle - \overline{T}| \sim \sigma_T\sqrt{\frac{t_f}{t}}, \tag{6}$$

which may be used to estimate how long we need to run a simulation before we can expect the running time average of the torque to converge to a well defined value (i.e. when the fluctuation estimate from equation 6 becomes significantly less than $|\overline{T}|$). Inspection of figure 7 suggests that the t_f is is typically about one half of a planetary orbit, $P_p/2$. Equation 6 tells us that the larger the relative amplitude of fluctuations, the longer we have to integrate for the running mean to converge.

It is clear that the level of fluctuations associated with the torques is very much larger than the running mean in figure 7. If we take the mean value of the torque to be $\overline{T} \simeq 9\times10^{-7}$ from the straight line in fig 7, then the typical magnitude of the fluctuations can be estimated to be $\sigma_T \simeq 2\times10^{-5}$, but with extreme fluctuations being a factor of ~ 40 times larger than the mean during certain periods of the evolution. If we set $\sigma_T \simeq 2\times10^{-5}$, then the expected time for convergence is approximately 250 planetary orbits. This time scale is much longer than the time over which it is feasible to run simulations of this kind at the present time, and may provide at least a partial explanation of why

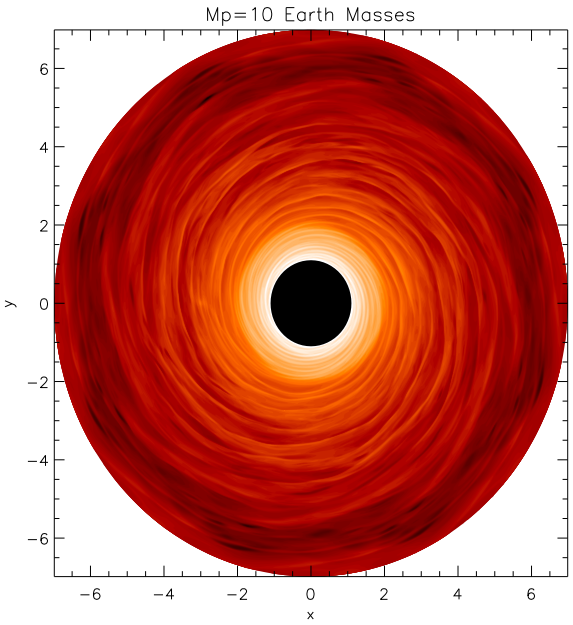

Figure 9. This figure shows midplane density contours for the run G2. Note that the presence of the protoplanet is just detectable although the perturbations generated by the turbulence are of higher amplitude than those generated by the protoplanet. The protoplanet is located at (x_p,y_p)= (-3,0).

convergence is not obtained in figure 8. But note that it may give a significant underestimate for the time required for convergence if the statistics of the fluctuations are more complex involving say a superposition of fluctuations with varying characteristic times up to the total evolution time of the global disc. In such a situation convergence to small means may be practically impossible.

3.3 Global Model G2

The protoplanet mass in this case was equivalent to $\simeq 10$ Earth masses. A snap shot of the midplane density distribution generated by run G2 is shown in figure 9. The presence of the protoplanet is just discernible at (x, y)= (-3.,0). Close up images of the density field in the vicinity of the protoplanet are shown in figure 10, and again the presence of the protoplanet can just be detected along with the spiral waves excited by the protoplanet. The time variability of the density field close to the protoplanet is apparent in this figure. Figure 11 shows the density field in the vicinity of the protoplanet in a laminar disc run that is otherwise equivalent to run G2, and it is worth noting that the density field shown in figure 11 remains essentially time independent once established.

Figure 12 shows the torque per unit mass as a function of time for a laminar run equivalent to G2. The approximate constancy of the middle line in this plot (which is the total torque per unit mass on the protoplanet) shows that a well defined torque and migration time can be ascribed in this case. Figure 13 shows an equivalent plot for run G2. As in run G1, the torque evolution in this case is characterised by large fluctuations about a small mean, such that the orbital

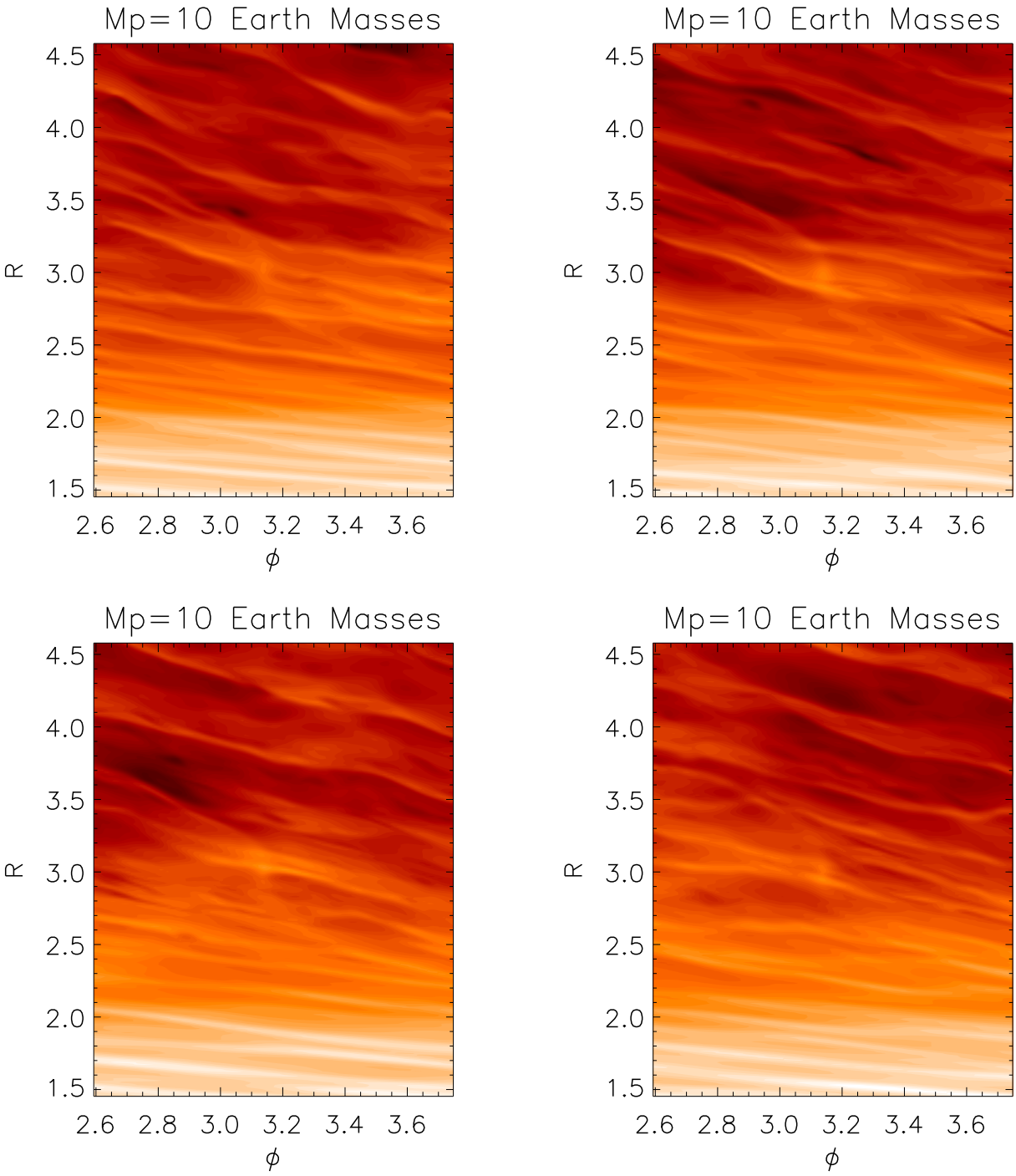

Figure 10. This figure shows midplane density contours for the run G2 in the region close to the protoplanet. The protoplanet is located at $(r_p,\phi_p)= (3,\pi)$. The panels correspond to times 429.0687, 496.8698, 542.0710, and 634.4136, respectively. Note that the presence of the protoplanet is just detectable, although the perturbation it makes to the disc is of lower amplitude than the perturbations generated by the turbulence.

evolution of the protoplanet is likely to occur as a random walk.

The running time average of the torques for run G2 are plotted in figure 14. The time average of the total torque is again found to not converge, showing variations that indicate inward migration on average after $\simeq$ 7 orbits have elapsed, outward migration on average after $\simeq$ 18 orbits, and inward migration on average again at the very end of the simulation. Using similar arguments presented in section 3.2 to estimate the time for the running mean to converge, we again estimate that the run time required will be around 70 – 80 planet orbits. This is significantly more than

the run time over which we are able to compute these models at the present time. However, the torques from the two sides of the disc exhibit somewhat relatively smaller amplitude fluctuations when compared to simulation G1. This is reflected in the shorter time estimated for convergence. It is also part of a tendency to have smaller relative fluctuations for larger protoplanet masses which makes net torque measurement easier. The same trend is seen in the shearing box simulations (see below). We also comment that the typical magnitude of the average torques from each side of the disc corresponds to the laminar value even in the low mass cases in spite of the large noise levels.

Although that may be the case, large noise levels which apparently can occur on a variety of time scales will cause the migration of a low mass protoplanet embedded in a turbulent disc to differ substantially from that found in a laminar disc model, with periods of inward migration interspersed with outward migration. At this present time we are unable to give a reliable estimate of the net migration time of protoplanets in such disc models, or because there may be significant variations occurring on the longest evolutionary time scales of the global disc, give even a reliable indication of the direction of migration in the long term. Feedback of the orbital evolution on the turbulence may be significant in some cases. Numerical experiments are currently being performed to examine this and will be the subject of a future publication.

In a recent paper, Winters, Balbus, & Hawley (2003a) have emphasised the 'chaotic' nature of MHD turbulence, with the implication being that the evolution of the turbulent state may be modified by small perturbations. The presence of a protoplanet induces such perturbations. Both simulations G1 and G2 were initiated with identical disc models (but not run G3), as commented upon in paper III. In paper III we noted that the global magnetic energy of the system was found to diverge (by a modest amount) once the planets had been inserted in the disc models. By comparing figure 7 with 13, and 8 with 14, we can see the affect that the differing planet masses have on the local statistics of the turbulence. While the overall magnitude and form of the torque fluctuations are similar, the details are clearly different. Given that these fluctuations appear to strongly influence the orbital evolution of the protoplanets, we can conclude that the detailed orbital evolution of a low mass protoplanet in a turbulent disc is essentially indeterminate due to the feedback between the turbulence and the planetary perturbations. Interestingly enough though, we can say that even if the mean average torque results in inward migration within a corresponding expected lifetime in the disc, large random fluctuations will result in some increased survival probability for such a time for a subset of an ensemble of protoplanets.

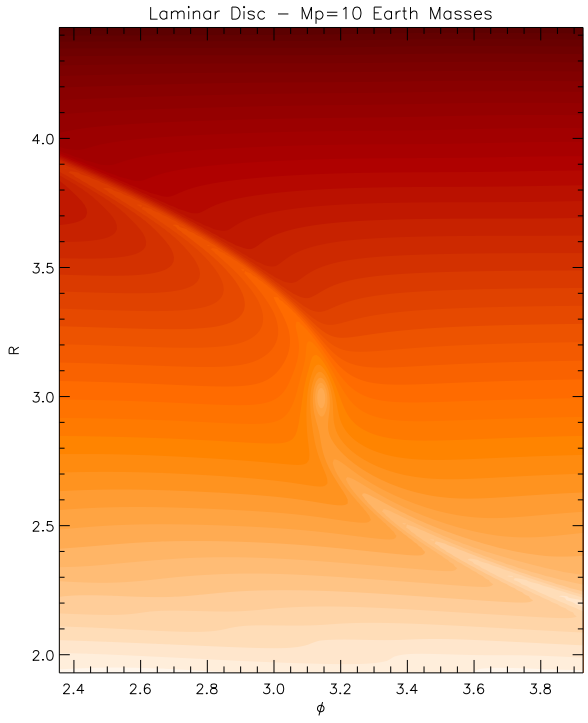

Figure 11. This figure shows midplane density contours for a laminar disc run with planet parameters identical to run G2. This figure should be compared with figure 10.

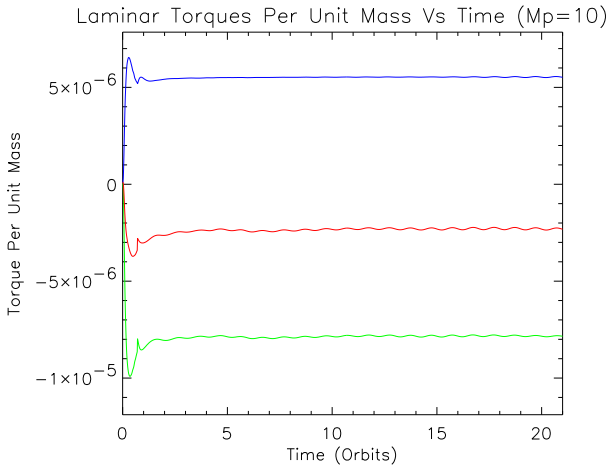

Figure 12. This figure shows the torque per unit mass exerted by the disc on the protoplanet for a laminar disc and planet parameters identical to run G2. The upper line shows the torque due to the inner disc, the lower line shows the torque due to the outer disc, and the middle line shows the total torque. It is clear that a well defined torque is produced, with an associated migration time scale.

3.4 Global Model G3

Figure 15 shows a snap shot of the midplane density structure in model G3, for which the protoplanet mass is equivalent to 30 Earth masses. The protoplanet is located at (x,y)=(-3.,0), and is clearly visible, along with the spiral waves it has generated. Figure 16 shows a series of close–up images of the midplane density near the protoplanet. Although the protoplanet and spiral waves it generates are clearly visible, it is also apparent that the density structure near the planet is highly variable. A close–up image of the density near the protoplanet for an equivalent laminar disc run is shown in figure 17 for comparison. The density field and spiral wakes in this case are essentially time independent.

The torque per unit mass as a function of time is shown

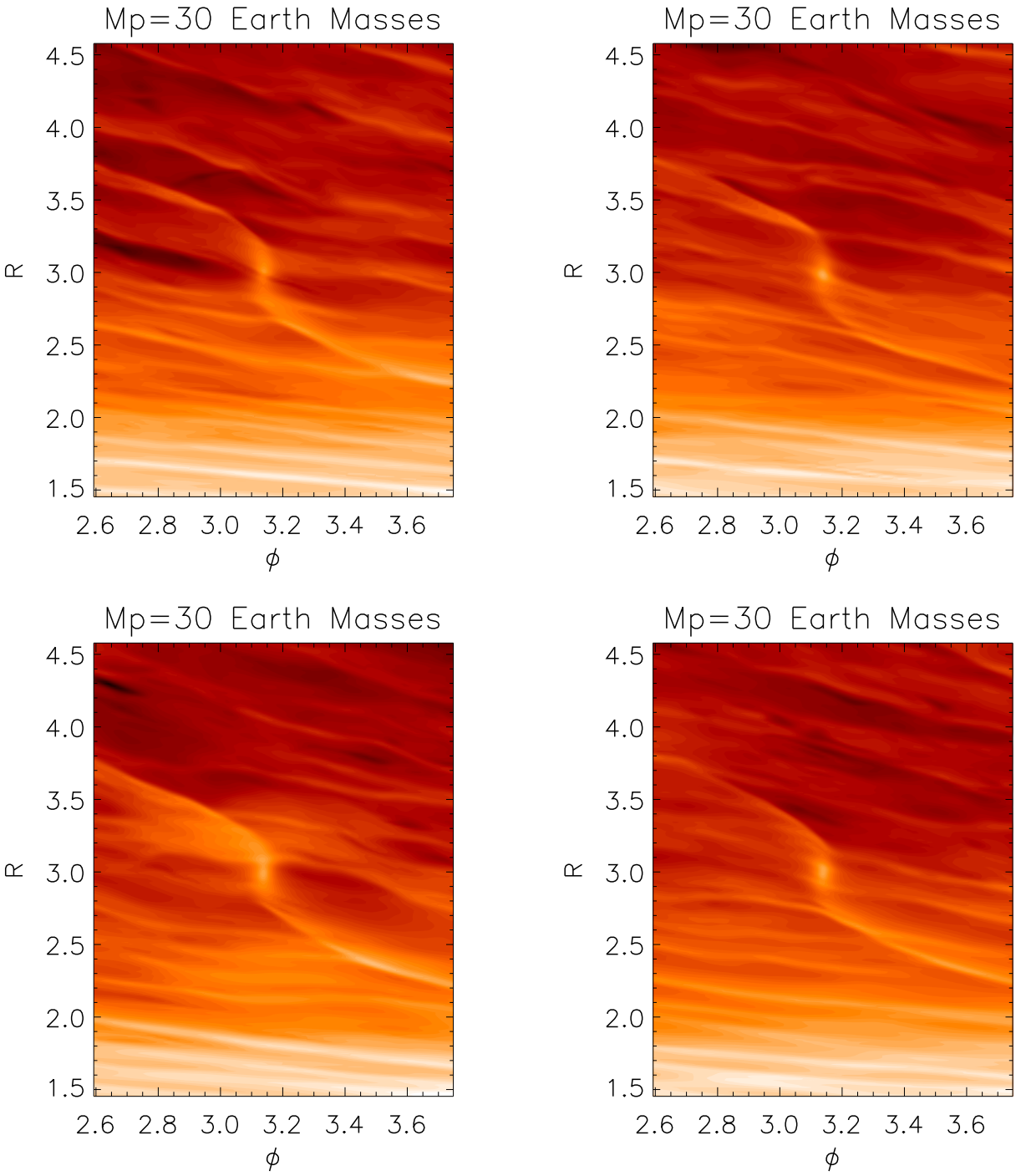

Figure 16. This figure shows midplane density contours for the run G3 in the region close to the protoplanet. The protoplanet is located at $(r_p,\phi_p)= (3,\pi)$. The panels correspond to times 871.4805, 903.0731, 948.2260, and 1077.837, respectively. Note that the presence of the protoplanet is clearly detectable, with the perturbation it makes to the disc being of similar amplitude to the perturbations generated by the turbulence. Note that the appearance of the spiral waves generated by the protoplanet are time variable since they are perturbed by the turbulence.

in figure 18 for the laminar disc run equivalent to run G3. The middle line shows the net torque per unit mass, whose approximate constancy leads to a well defined migration time. The time evolution of the torque per unit mass for run G3 is shown in figure 19. A similar situation to that described for runs G1 and G2 is observed, with the torques being significantly modified by strong fluctuations. Again the total torque can be seen to show periods of being positive and negative, suggesting that the protoplanet would

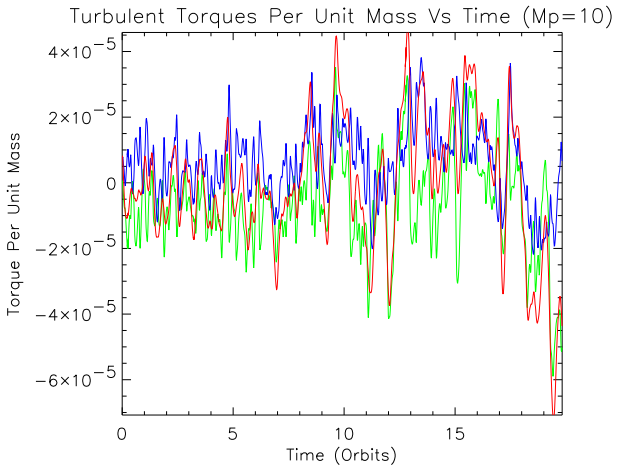

Figure 13. This figure shows the torque per unit mass exerted by the disc on the protoplanet for the run G2. The turbulence in this case generates strong fluctuations in the torque from each side of the disc, such that it becomes difficult to distinguish the torques arising from each side. The total torque fluctuates between positive and negative values such that the associated migration will undergo a 'random walk'.

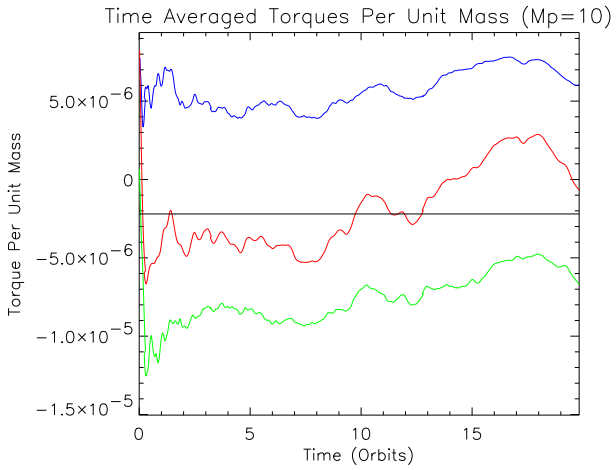

Figure 14. This figure shows the running time average of the torque per unit mass exerted by the disc for run G2. The upper line is the running time average of the torque acting on the planet due to the inner disc. The lower line is that due to the outer disc. The middle (not straight) line is the running time average of the total torque. The straight line is the total torque exerted on the protoplanet in a laminar disc run. We note that the total time averaged torque does not converge to a well defined value.

undergo a random walk rather than monotonic, inward migration.

We note, however, that as the protoplanet mass increases, and the spiral waves excited increase in amplitude to become comparable or larger that the turbulent density wakes, the torques due to the inner and outer disc begin to separate. This can be observed by comparing figures 7, 13, and 19, which show the torques from the inner and outer discs becoming progressively distinguishable from each other as the planet mass increases. This is also accompanied by a reduction in the relative torque fluctuation noise level.

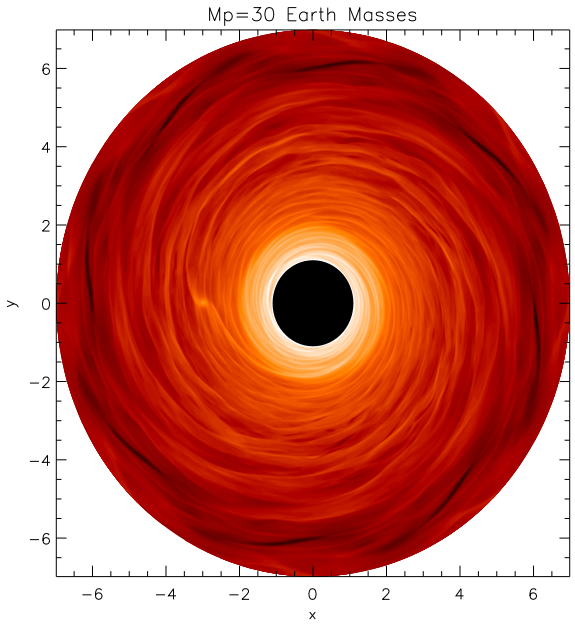

Figure 15. This figure shows midplane density contours for the run G3. The presence of the protoplanet is clearly detectable, with the perturbations generated by the protoplanet being of similar magnitude to those generated by the turbulence. The protoplanet is located at (x_p,y_p)= (-3,0).

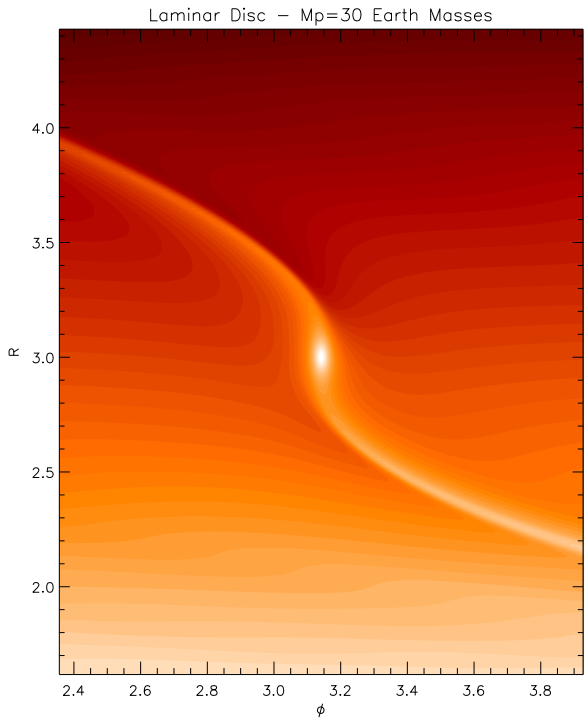

Figure 17. This figure shows midplane density contours for a laminar disc run with planet parameters identical to run G3. This figure should be compared with figure 16.

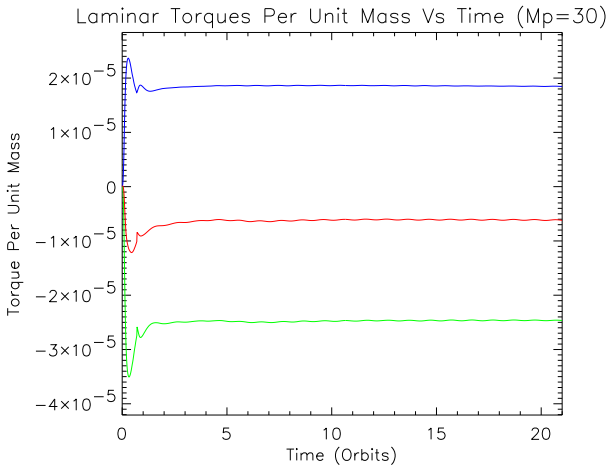

Figure 18. This figure shows the torque per unit mass exerted by the disc on the protoplanet for a laminar disc and planet parameters identical to run G3. The upper line shows the torque due to the inner disc, the lower line shows the torque due to the outer disc, and the middle line shows the total torque. It is clear that a well defined torque is produced, with an associated migration time scale.

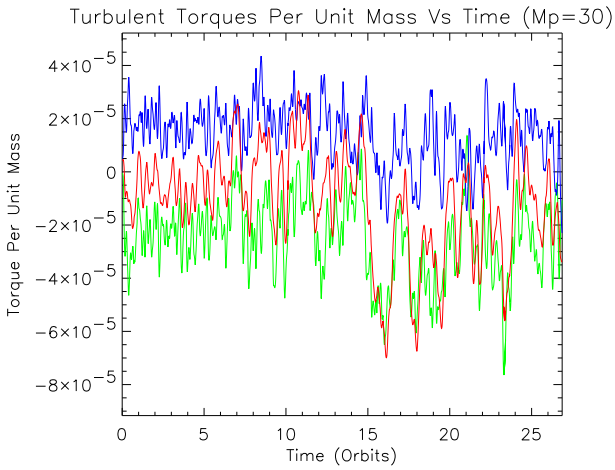

Figure 19. This figure shows the torque per unit mass exerted by the disc on the protoplanet for the run G3. The turbulence in this case generates strong fluctuations in the torque from each side of the disc, such that it becomes difficult to distinguish the torques arising from each side. The total torque fluctuates between positive and negative values such that the associated migration will undergo a 'random walk'.

Figure 20 shows the running time average of the torques per unit mass for run G3. The straight line in this figure is the time averaged total torque per unit mass obtained in the equivalent laminar disc run. As in runs G1 and G2, the running time average of the total torque per unit mass fails to converge for the run time considered here. However, the relative fluctuation amplitudes are smaller in this case leading to a smaller anticipated time for convergence. This is part of the trend for larger mass protoplanets to produce larger amplitude perturbations that are more difficult for the turbulence to affect.

If we consider the running mean of the total torque in

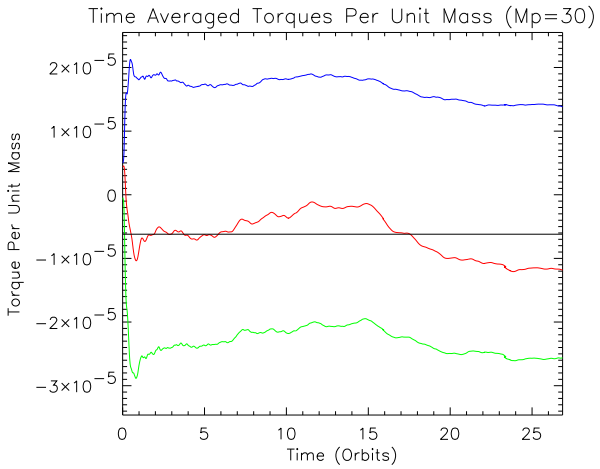

Figure 20. This figure shows the running time average of the torque per unit mass exerted by the disc for run G3. The upper line is the running time average of the torque acting on the planet due to the inner disc. The lower line is that due to the outer disc. The middle (not straight) line is the running time average of the total torque. The straight line is the total torque exerted on the protoplanet in a laminar disc run. We note that the total time averaged torque does not converge to a well defined value.

figure 20 we can reasonably take a value of $\overline{T} \simeq -6 \times 10^{-6}$. A by–eye inspection of figure 19 indicates that the level of fluctuation in the torques is $\sigma_T \simeq 4 \times 10^{-5}$. The predicted run time for convergence of the running mean from equation 6 is then $\simeq 20 - 30$ planetary orbits, which is shorter than for G1 or G2 and is comparable to the time for which the simulation has been run.

Although it always corresponds to inward migration, the non convergence of the running mean toward a well defined value suggests that a simple picture of local turbulence in the vicinity of the planet, in which the state variables have well defined mean values on top of which are superposed fluctuations with a well defined Gaussian spectrum, is not accurate. Instead, it appears that the global nature of the disc plays an important role in continuously modifying the local structure of the disc and turbulence. Communication between different regions of the disc can affect the local properties such as the mean density, the amplitude, spatial, and temporal distribution of density and velocity fluctuations over long time scales, such that a local running mean is problematic to define. An examination of the global properties of a turbulent disc model, such as the global magnetic energy (see e.g. papers I–III) show that there are short and longer time scale variations in the turbulence that reflect modifications to the local and global turbulence, and by implication the local disc structure. The results presented in section 3.6 for the local shearing box simulations show smaller relative fluctuations and greater convergence of the mean torques toward the expected value, indicating that the global properties of turbulent discs may play an important role by inducing longer time scale modification to the local state of the disc in the vicinity of an embedded protoplanet.

3.5 Global Run G5

The planet mass in global run G5 was equivalent to 3 Jupiter masses. The computational domain in this case was restricted so that the azimuthal interval ran between $[0, \pi/2]$ (thus allowing a reasonable run time), with the protoplanet being placed on a fixed circular orbit at $(r_p, \phi_p) = (2.5, \pi/4)$. The physical parameters were identical to run G4, for which the azimuthal domain covered the full 2π. However, run G4 was only run for $\simeq 11$ planetary orbits, which is too short a time for anything other than the tendency for gap formation and the global disc morpholgy to be inferred. Consequently run G4 will not be discussed further here.

Run G5 has been described in paper III, and showed a tendency toward clear gap formation with the response of the disc due to the presence of the planet being strongly non linear. Consequently the perturbations induced in the disc by the protoplanet are very much larger than those that arise because of the turbulence. This results in the fluctuations in the torque experienced by the protoplanet being significantly smaller (in relative terms) than observed in the previously described runs G1, G2, and G3, and a well defined running time average of the torque being obtained. Figure 21 shows the running time average of the torque per unit mass obtained from run G5, with the upper line corresponding to the inner disc torque, the lowest line corresponding to the outer disc torque, and the middle line the running time average of the total torque. It is clear from this figure that a large torque is exerted on the protoplanet prior to gap formation, but that as the gap proceeds to open and material is pushed away from the planet the torque diminishes. The running time averaged torques due to the inner and outer disc appear to be approaching well defined asymptotic values, which are unaffected by turbulent fluctuations, but the continued decrease in the running time averages indicates that gap formation is still ongoing at the end of the simulation.

We note that the use of a closed inner boundary in this simulation, combined with the close proximity of the planet to the inner boundary, cause the density of the inner disc to be maintained at an artificially high level after gap formation. This leads to the net torque on the planet being negative but close to zero. Under more general circumstances in which the inner disc can accrete onto the central star, an inner cavity is expected to form such that the torque on the protoplanet is dominated by the outer disc (e.g. Nelson et al. 2000). If we adopt the disc model described in section 3.1 used to normalised the results presented in figure 2, and estimate the migration time using equation 2 and a torque per unit mass due to the outer disc in figure 21 of $T = -10^{-5}$, then we obtain $\tau_{mig} \simeq 4 \times 10^4$ yr, for a planet at 5.2 AU. The type II migration time appropriate to gap forming protoplanets is given by the viscous evolution time $\tau_{mig} = (2r_p^2)/(3\nu)$ where $\nu = \alpha H^2 \Omega$ is the kinematic viscosity. For a disc model with $\alpha \simeq 7 \times 10^{-3}$ and $H/r = 0.07$, the estimated type II migration time is $\tau_{mig} = 4.5 \times 10^4$ yr, in reasonable agreement with the result obtained from the simulation G5.

We note that the above estimates for type II migration times correspond to disc models with full 2π azimuthal domains, and that it is unclear which precise value the running mean of the outer disc torque will approach once gap formation is complete. Nonetheless, the reasonable agreement obtained in the estimates suggests that gap forming protoplanets in turbulent discs undergo migration at the expected type II rate. A similar result was obtained in paper II for type II migration rates in turbulent discs with full 2π azimuthal domains.

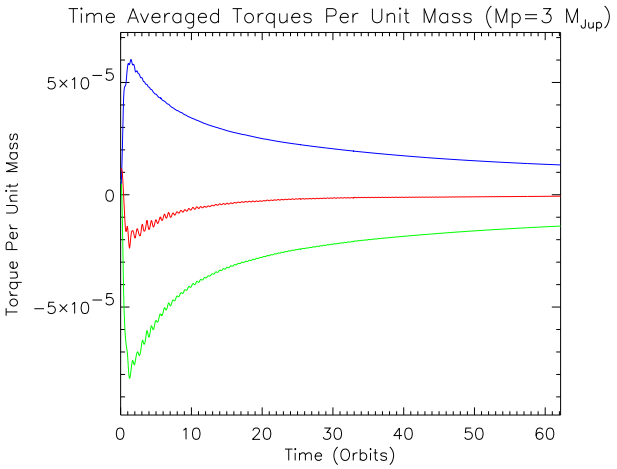

Figure 21. This figure shows the running time average of the torque per unit mass exerted by the disc for run G5. The upper line is the running time average of the torque acting on the planet due to the inner disc. The lower line is that due to the outer disc. The middle line is the running time average of the total torque. The running time average for both the outer and inner torque converge to well defined values in this run, for which the interaction is non linear and the planet opens up a large gap. We note that our use of a closed inner boundary causes the density of the inner disc to be artificially increased after gap formation, such that the torque due to the inner disc is probably an over estimate, leading to a larger torque contribution.

It is clear that a well defined trend arises when considering the interaction between embedded protoplanets and turbulent discs. Lower mass objects that are unable to perturb the turbulent background flow significantly are subject to strong torque fluctuations that are likely to dominate their orbital evolution. As the protoplanet mass increases so that the amplitude of the spiral wakes that it excites become larger than the turbulent density fluctuations, the relative magnitudes of the torque fluctuations decrease, and the migration is likely to become similar to type I migration (although with a significant noise component). For larger protoplanet masses that allow gap formation, the effect of the turbulent fluctuations is small, with the migration being essentially the same as the standard type II picture. These trends are also observed in the shearing box simulations that are described below.

3.6 Shearing Box Simulation Results

Details of the shearing box simulations Ba1 - Ba4 are given in table 2. These were each continued from a simulation with fully developed turbulence Ba0 after inserting a protoplanet with values of the dimensionless parameter $GM_p/(H^3\Omega_p^2) = M_p R^3/(M_* H^3)$ measuring the mass of the protoplanet equal to $0.1, 0.3, 1$ and 2 respectively. In this section, Ω_p and R are the angular velocity and radius of

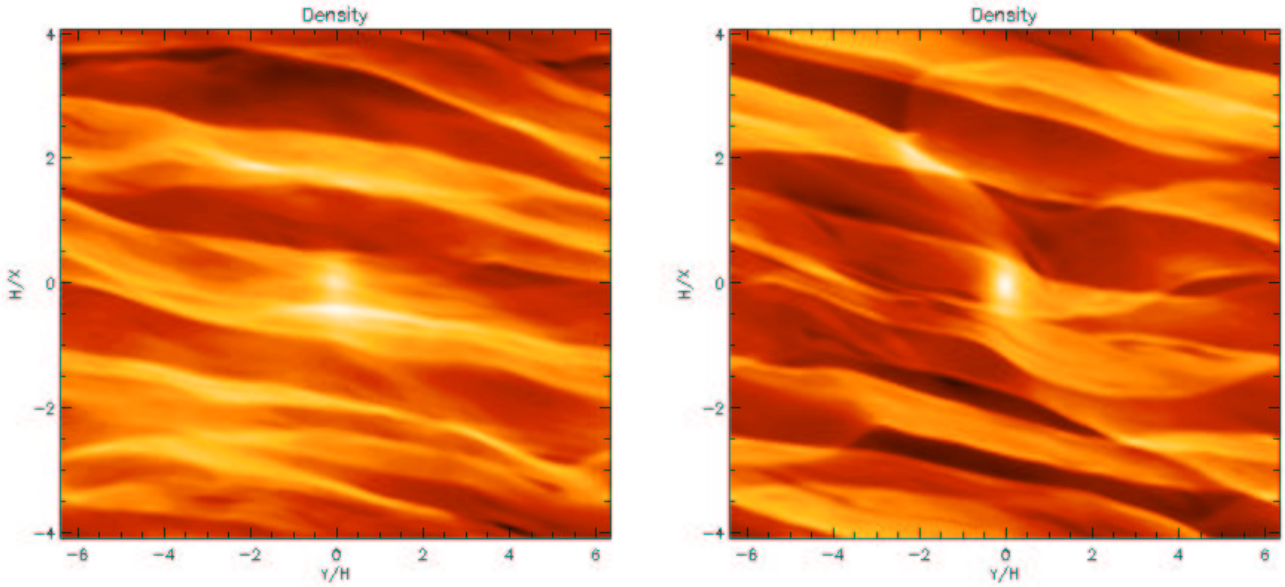

Figure 22. Density contour plots taken in the box mid plane for simulations Ba1 and Ba2 which have the smaller mass and hence fully embedded protoplanets. The wakes produced by these protoplanets can be discerned even though the medium is turbulent.

the centre of the box. Thus simulations Ba1 and Ba2 are directly comparable to the global simulations G2 and G3 in terms of the relative strength of the protoplanet's perturbation on the disc. As in those cases the protoplanets remain embedded with no indication of gap formation. However, simulations Ba3 and Ba4 show gap formation and a non linear perturbation of the disc as do simulations G4 and G5. We here discuss the force exerted on the protoplanet by the disc. In particular we study the component in the azimuthal direction F_y. Adopting a unit of length equal to the radius of the center of the box, this is also the torque.

Density contour plots taken in the box mid plane near the end of the simulations Ba1 and Ba2 which have embedded protoplanets are shown in figure 22. As in the global simulations, the wakes produced by these protoplanets can be discerned even though the the medium is turbulent and produces erratic perturbations of them. Thus the tidal perturbation of the disc produces measurable effects.

Figure 23 shows running time averages of the torques acting on the protoplanet in simulations Ba1–Ba4. Apart from simulation Ba1, these commence from when the protoplanets were introduced into the simulations. In the case of Ba1, the running average was started somewhat later.

The averages were calculated over time periods of typically 50 orbits at the centre of the box. In each case the average torques from the regions exterior to and interior to the protoplanet drag and accelerate the protoplanet as expected. Although, as in the global simulations, fluctuations in the one sided torques can be very large amounting to an order of magnitude or more greater than the typical average value, the averages tend to approach reasonably steady values. Note that in a shearing box, symmetry considerations require that the mean torques from the two sides of the disc should ultimately be equal and opposite. However, some noise remains even after fifty orbits. The noise is stronger in the embedded cases and remains at the five to ten percent level after fifty orbits. The resulting mean net torque which would be zero in a laminar simulation suffers corresponding fluctuations. However, the effects of noise seems much less severe in simulations Ba3 and Ba4 in which the disc is non linearly perturbed, in agreement with the global run G5. In these cases turbulent fluctuations seem to be less able to modulate the torque estimates and non zero net torques arising from features added to bias the box are more readily measurable.

To illustrate the reduced effects of noise on the simulations with strongly perturbing protoplanets, we compare running time averages of the torques acting on the protoplanet in simulation Ba4 with those obtained from the corresponding laminar disc simulation in figure 24. The averages commence from when the protoplanet was introduced. Corresponding plots from the two simulations are very similar. Note that the torques tend to relatively weaken at later times in the laminar case. This is because this simulation with $(M_p R^3/(M_* H^3) = 2$ produces a wider and deeper gap than the turbulent case (see paper III). This in turn results in less matter for the protoplanet to interact with locally on average and hence weaker average torques at later times.

Finally we comment on the magnitudes of the time averaged one sided torques. As for the global runs these are similar for turbulent and corresponding laminar disc simulations. For the shearing box simulations, the fiducial value expected for the one sided linear torques in the 2D laminar case with no potential softening is

$$F_{y0} = 0.4\pi\Sigma R^3 \Omega_p^2 \left(\frac{M_p^2 R^3}{M_* H^3}\right), \qquad (7)$$

where the surface density $\Sigma = \langle\rho\rangle H$, with $\langle\rho\rangle$ being the volume and time averaged density in the box (see Ward 1997). For simulation Ba1, $F_{y0} = 10^{-13}$ in our computational units making the typical averaged torques about fifty percent of the fiducial value. Such a reduction may occur as a result of softening the gravitational potential due to the protoplanet (see section 3.1 and paper III). This would indicate

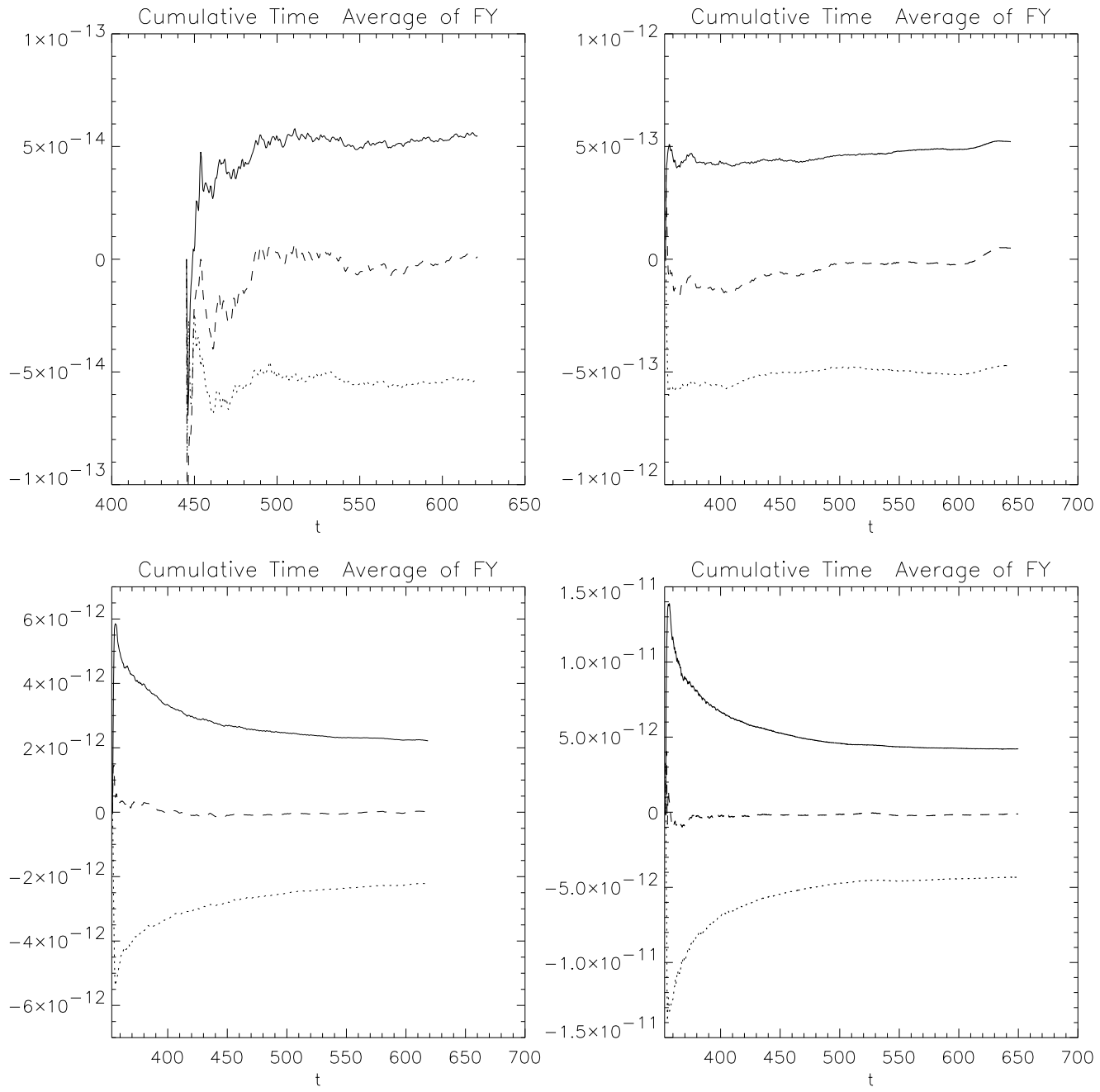

Figure 23. This figure shows running time averages of the torques acting on the protoplanet in simulations Ba1 top left panel, Ba2 top right panel, Ba3 bottom left panel and Ba4 bottom right panel. In each panel the upper lower and middle curves correspond to running averages of the torques acting on the planet due to the regions of the box interior to the planet, the torque due to the regions exterior to the planet, and the net torque respectively.

that the magnitude of the torques is essentially given by the laminar disc theory. However, the turbulence adds a significant noise component when the protoplanet mass is small enough to place the response in the linear regime. We comment that the averaged torque magnitudes in Ba1 and Ba2 are consistent with a scaling $\propto M_p^2$ appropriate to the linear response regime but that the torque is weaker than suggested by such a scaling in Ba3 and Ba4. This is consistent with the response being non linear in those cases.

4 DISCUSSION

In this paper we have performed both global and local simulations of embedded protoplanets interacting with a turbulent disc and studied the behaviour of the torques exerted between the disc and protoplanets and the consequences for orbital migration. The global simulations were for a disc with $H/r = 0.07$ that exhibited MHD turbulence with zero net magnetic flux with mean $\alpha \sim 0.007$. The protoplanet masses considered were $M_p = 3, 10$ and 30 Earth masses,

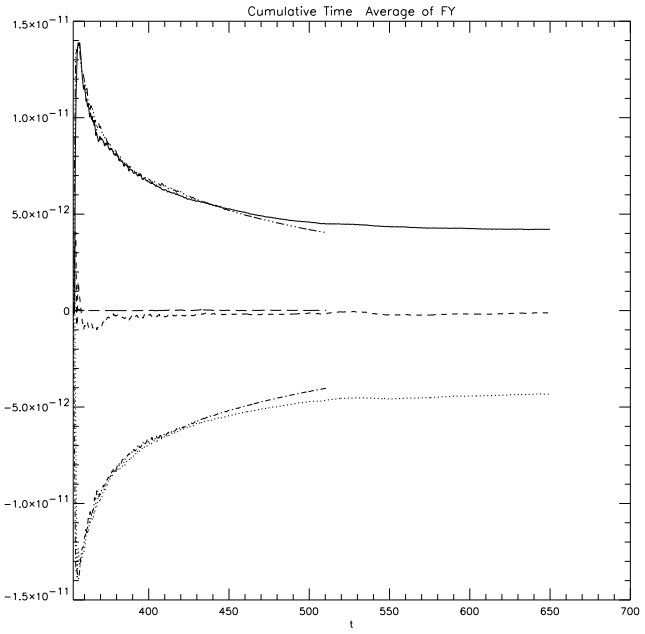

Figure 24. This figure shows running time averages of the torques acting on the protoplanet in simulation Ba4 commencing from when the protoplanet was introduced. The uppermost curve extending to larger times gives the net torque acting on the planet from the inner regions while the corresponding lowermost curve gives the contribution from the outer regions. The central short dashed curve gives the net torque. For comparison results from a laminar simulation with the same parameters but no magnetic field are presented. Corresponding plots from the two simulations can be almost superposed but the laminar case terminates at an earlier time.

and 3 Jupiter masses. The local shearing box simulations can be characterized by values of the dimensionless parameter $M_p R^3/(M_* H^3)$. The simulations adopted $0.1, 0.3, 1.0$, and 2.0 respectively. The first two of these are directly comparable to the global simulations with $M_p = 10 M_\oplus$, and $M_p = 30 M_\oplus$ respectively. The latter two have gap forming protoplanets, but whose masses correspond to less massive planets than the 3 Jupiter mass planet considered in the global run G5, and enable the behaviour of the torques in the non linear gap forming regime to be studied. For a first study, the protoplanets considered here were held in fixed circular orbit.

It was always found that the instantaneous torque experienced by a protoplanet was a highly variable quantity on account of the protoplanet interacting with the turbulent density wakes that shear past it. For low mass protoplanets that are not able to begin to form a gap, the torque is dominated by these fluctuations, such that at any particular time, the usual distinction between inner (positive) and outer (negative) disc torques is blurred. The net torque experienced by embedded protoplanets oscillates between negative and positive values, such that the protoplanet migration is likely to occur as a random walk. This is in contrast to the monotonic inward drift normally associated with type I migration.

In order to average out the erratic behaviour of the instantaneous torque a running time average is considered. We considered contributions from the inner and outer disc. We have been able to do this over a 20 orbital period timescale. Although these running averages took on values characteristically expected for type I migration, large fluctuations remained such that the net torques failed to converge to well defined values over the run times that are currently feasible. This is in contrast to laminar disc simulations for which convergence is achieved on an orbital time scale.

Fluctuations in the averaged one sided and net torques were most severe for the smaller embedded masses. Thus for the $3 M_\oplus$ global simulation, fluctuations in the one sided torques averaged over ~ 20 orbits were comparable to the averaged torques themselves resulting in an indeterminate direction of migration. However, in the case of the $30 M_\oplus$ global simulation, fluctuations in the one sided averaged torques were relatively smaller at about 20 percent of the mean values resulting in a more clearly delineated but still erratic inward migration.

The existence of large fluctuations in the torques exerted by the disc on embedded low mass protoplanets and lack of knowledge of how these behave on long time scales makes definitive statements about the direction and rate of migration difficult to make. However, even in spite of large instantaneous fluctuations of more than one order of magnitude larger than the mean values, characteristic values of one sided torques averaged over a 20 orbit time scale are consistent with laminar type I estimates. Thus, when this estimate gives inward migration to the central object, we might expect the fluctuations to result in increased survival prospects for a subset of a statistical ensemble of embedded protoplanets.

The behaviour of the fluctuations on long timescales remains an important issue that is impractical to explore at the present time. If there are significant fluctuations generated in the global simulations that occur on the longest evolutionary time scales, convergence of torque running means becomes for practical purposes impossible to achieve and the migrational behaviour of low mass protoplanets considered as an ensemble would be very different from predictions of type I migration theory.

We found that noise levels were relatively smaller in the local shearing box simulations. This gives some support to the idea of the existence of global fluctuations with long characteristic times in the global simulations which are expected to be absent in the box simulations.

We comment that the zero net magnetic flux models that we consider here generally give rise to turbulent discs that are more quiescent than those which arise when the magnetic fields has net flux, especially if a net poloidal field is present (e.g. Hawley, Gammie, & Balbus 1996; Hawley 2001; Steinacker & Papaloizou 2002). Strong density fluctuations and contrasts, including persistent gaps, may arise in such discs, and would have a profound impact on the migration of embedded protoplanets. In particular, if MHD turbulence gives rise to global disc structures that lead to varying migration rates as a function of position in the disc, then migration of embedded protoplanets into these low–migration regions is likely to occur, increasing the lifetime of these planets in the disc.

The results of both the global and local simulations show the same trend as a function of planet mass. For very low mass protoplanets the turbulent density wakes have higher amplitude than the spiral wake generated by the pro-

toplanet. The torques exerted on the protoplanet are then such that the instantaneous turbulent fluctuations are very much larger than the running means. However, as the planet mass increases, the perturbation it makes on the disc starts to dominate its local neighbourhood. The expected separation between inner and outer disc torques becomes apparent and fluctuations become smaller relative to the running mean torques. Eventually gap formation occurs. At this point we find a weakening of the torques exerted by the disc on the protoplanet due to the evacuation of gap material. There is then a transition to type II migration at a rate determined by the angular momentum transport in the distant parts of the disc unaffected by the protoplanet. This has already been seen in the simulation of a 5 Jupiter mass protoplanet described in paper II.

4.1 Acknowledgements

The computations reported here were performed using the UK Astrophysical Fluids Facility (UKAFF).

REFERENCES

Armitage, P. J., 1998, ApJ, 501, L189
Balbus, S. A., Hawley, J. F., 1991, ApJ, 376, 214
Bate, M.B., Lubow, S.H., Ogilvie, G.I., Miller, K.A., 2003, MNRAS, 341, 213
Bodenheimer, P., Pollack, J.B., 1986, *Icarus,* 67, 391
Boss, A.P., 2001, ApJ, 563, 367
Brandenburg, A., Nordlund, Å., Stein, R. F., Torkelsson, U., 1996, ApJ, 458, L45
Bryden, G., Chen, X., Lin, D. N. C., Nelson, R. P., Papaloizou, J. C. B., 1999, ApJ, 514, 344
D'Angelo, G.; Henning, T.; Kley, W., 2002, A&A, 385, 647
Gammie, C.F., 1996, ApJ, 457,355
Goldreich, P., Tremaine, S., 1979, *ApJ,* 233, 857
Hartmann, L., Calvet, N., Gullbring, E., D'Alessio, P., 1998, ApJ, 495, 385
Hawley, J. F., 2000, ApJ, 528, 462
Hawley, J. F., 2001, ApJ, 554, 534
Hawley, J.F., Balbus, S.A., 1991, ApJ, 376, 223
Hawley, J. F., Gammie, C. F., Balbus, S. A., 1996, ApJ, 464, 690
Hawley, J. F., Stone, J. M., 1995, Computer Physics Communications, 89, 127
Hawley, J. F., 2000, ApJ, 528, 462
Hawley, J. F., 2001, ApJ, 554, 534
Kley, W., 1999, MNRAS, 303, 696
Lin, D.N.C., Papaloizou, J.C.B., 1979, MNRAS, 186, 799
Lin, D.N.C., Papaloizou, J.C.B., 1986, ApJ, 309, 846
Lin, D.N.C., Papaloizou, J.C.B., 1993, Protostars and Planets III, p. 749-835
Lubow, S.H., Seibert, M., Artymowicz, P., 1999, ApJ, 526, 1001
Marcy, G. W., Cochran, W. D., Mayor, M., 2000, Protostars and Planets IV (Book - Tucson: University of Arizona Press; eds Mannings, V., Boss, A.P., Russell, S. S.), p. 1285
Mayor, M., Queloz, D., 1995, Nature, 378, 355
Nelson, R.P., Papaloizou, J.C.B., 2003a, MNRAS, 339, 993 – Paper II
Nelson, R. P., Papaloizou, J. C. B., Masset, F., Kley, W., 2000, MNRAS, 318, 18
Papaloizou, J.C.B, Lin, D.N.C., 1984, ApJ, 285, 818
Papaloizou, J.C.B., Nelson, R.P., 2003, MNRAS, 339, 983 – Paper I
Papaloizou, J.C.B., Nelson, R.P., Snellgrove, M.D., 2003, MNRAS, submitted – Paper III
Pollack, J.B., Hubickyj, O., Bodenheimer, P., Lissauer, J.J., Podolak, M., Greenzweig, Y., 1996, *Icarus,* 124, 62
Santos, N.C., Israelian, G., Mayor, M., Rebolo, R., Udry, S., 2003, *A&A,* 398, 363
Shakura, N. I., Sunyaev, R. A., 1973, A&A, 24, 337
Steinacker, A., Papaloizou, J.C.B., 2002, ApJ, 571, 413
Tanaka, H., Takeuchi, T., Ward, W.R., 2002, ApJ, 565, 1257
Terquem, C.E.J.M.L.J., 2003, MNRAS, 341, 1157
Van Leer, B., 1977, *J. Comp. Phys.*, 23, 276
Vogt, S. S., Butler, R. P., Marcy, G. W.; Fischer, D. A.; Pourbaix, D., Apps, K., Laughlin, G., 2002, ApJ, 568, 352
Ward, W.R., 1986, *Icarus,* 67, 164
Ward, W.R., 1997, *Icarus,* 126, 261
Winters, W., Balbus, S., Hawley, J., 2003a, MNRAS, 340, 519
Winters, W., Balbus, S., Hawley, J., 2003b, ApJ, 589, 543
Ziegler, U., Rüdiger, G., 2000, A&A, 356, 1141